

Strong inertial currents and marginal internal wave stability in the central North Sea

Hans van Haren, Leo Maas, J.T.F. Zimmerman¹, Herman Ridderinkhof and Hans Malschaert

Netherlands Institute for Sea Research, Den Burg, the Netherlands

Abstract. Solar insolation *stabilizes* the water column and suppresses vertical exchange. Observations from the central North Sea clearly show that increased heating in summer is accompanied by enhanced *de-stabilizing* vertical current differences (shear), surprisingly to such extent that the equilibrium state is marginally stable. Under calm weather conditions, the shear is predominantly generated by near-inertial motions while the internal wave spectrum primarily results from nonlinear interaction between the dominating tidal and near-inertial motions. In terms of the associated enhanced vertical mixing across the largest vertical temperature gradients, shelf seas are not different from the abyssal ocean, despite the proximity to energy sources near boundaries in the former. By the lack of sufficiently strong wind- and tidal mixing this internal mixing is considered to be responsible for the diapycnal transport of nutrients leading to the observed increase in near-surface values and triggering the late-summer phytoplankton bloom.

Introduction

When the sun heats the sea in summer, the water column becomes stably stratified in density as temperature decreases with depth, warm water being less dense than cold water. In shelf seas, contrasting with the abyssal ocean, wind and tidal mixing concentrate the initially gradual temperature decrease into a thin layer, the thermocline. By its increased stability, the thermocline impedes vertical turbulent exchange. However, once present the two stably stacked mixed layers allow for the development of slab-like motion of either of the layers, yielding vertical current differences (shear), which tend to *enhance* vertical mixing across the thermocline [Munk and Anderson, 1948]. This is suggested to be due to their destabilizing effect on short internal waves which may grow until breaking [Garrett and Munk, 1972a; Gregg and Kunze, 1991].

Despite the strong (seasonal) stratification, year-long observations from the central North Sea [Ruardij et al., 1997] show a continuous increase in near-bottom temperature, which points at vertical exchange across the stratification at an average turbulent diffusive rate of $K = 4 \times 10^{-5} \text{ m}^2 \text{ s}^{-1}$, which is about 100 times larger than the molecular value and similar to previously reported deep basin values [Gregg and Kunze,

1991]. Such vertical mixing cannot be directly generated by wind and tidal mixing when the stratification is not concentrated in a very thin layer and, consequently, the two mixing layers do not overlap. In this paper we discuss the influence of varying stratification on currents, shear and associated mixing, and the role of internal waves therein. Because of similarity in these processes, shelf sea studies on internal waves and water column stability are of value for similar abyssal ocean studies.

Observations

Data are presented from the central North Sea at $54^\circ 25' \text{ N}$ and $04^\circ 02' \text{ E}$ where the water depth is about 45 m. The water temperature and, hence, stratification have been monitored from surface to bottom using 3 thermistor strings, each holding 10 or 11 thermistors, at 2 m intervals between 3-21 m depth and 31-43 m depth, and at 1 m intervals between 21-31 m depth. Current measurements at 0.5 m vertical increments have been obtained from a bottom mounted, upward looking 600 kHz RDI-broadband acoustic Doppler current profiler (ADCP).

In summer, the observed currents differ substantially from those observed in winter (not shown here), as the typical semi-diurnal tidal (M_2) current dominance is found only *below* the stratification [Figure 1(b)]. Above the bottom mixed layer, the tidal currents are superposed on motions of about equal magnitude, having a period of 14.7 hours, which corresponds to the local inertial frequency f . These (near-) inertial motions accompany the adjustment towards equilibrium on a rotating earth, as generated by a variety of disturbances such as a sudden shift of direction of a *moderate* wind on day 195 [Figure 1(a)]. However, most conspicuous is the vertical variation of these motions, with a 180° current reversal across both major thermoclines.

The associated vertical current shear ($S = [\partial u/\partial z, \partial v/\partial z]$, where u, v denote the horizontal current components at depth z), is thus much larger in summer than in winter, and closely related to the varying stratification rate. The possible destabilization of the water column by such shear is investigated by computing the gradient Richardson number $Ri = N^2/|S|^2$ [Turner, 1979]. Here, stability is represented by $N = \{-g \, d \ln \rho / dz\}^{1/2}$ the buoyancy frequency, with g the acceleration of gravity, pointing in the downward, negative z -direction and, using for the density variations $\delta \rho = -\alpha \delta T$, with T the temperature. The thermal expansion coefficient $\alpha \approx 0.2$ is evaluated from Seabird SBE-911 CTD-observations near the moorings, showing a monotonic T-S relationship and little contribution of salinity to large scale density variations.

Our data frequently show values of $Ri < 1$, and occasionally $Ri < 0.25$ [Figure 1(c)], which indicates that the flow is marginally stable, and subject to occasional bursts of

¹Also at Inst. Marine Atmos. Sci., Univ. Utrecht, the Netherlands.

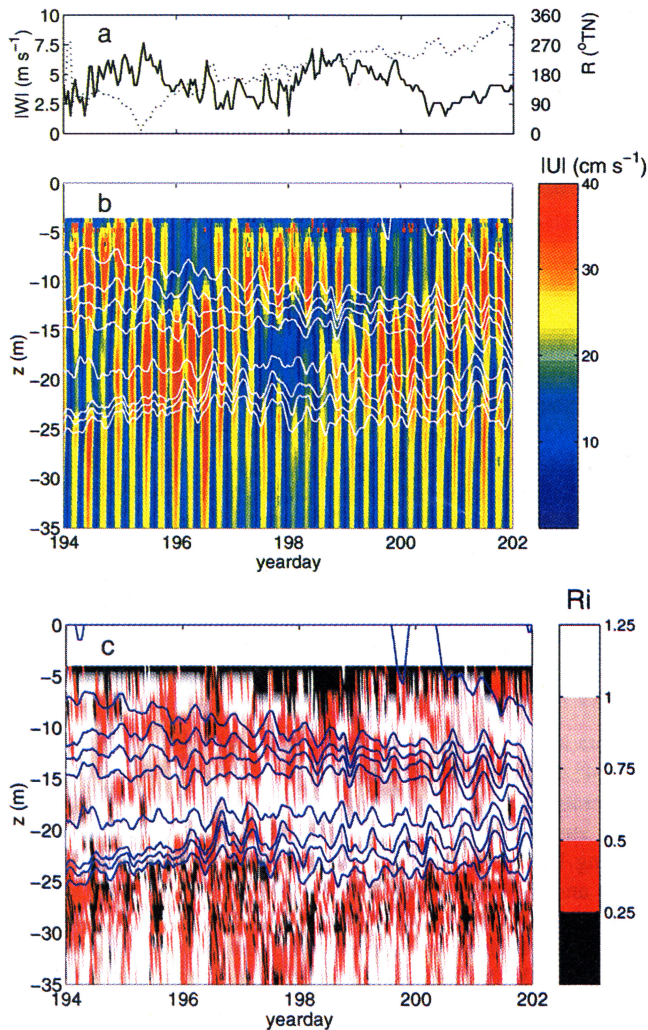


Figure 1. The summer stratification, as presented in each color panel by white or blue solid isotherms drawn every 1 °C, from 10–18 °C, and, (a) Wind speed (W , solid line) and direction (R , dotted line), which are observed at a platform located 150 km to the south-west of the mooring. (b) Total current amplitude (note the bad current observations above 5–8 m depth, due to side-lobe interference). Above 25 m depth the amplitude varies regularly with depth and time between about zero and 45 cm s^{-1} , a doubling of the tidal current amplitude (of 20–30 cm s^{-1}). The period of variation in time is 3.3 days, the M_2 - f beat period, and maxima and minima alternate in depth between the near surface well-mixed layer and the layer between the two major thermoclines, which are 2–5 m thick. Below 35 m the pattern is as between 25–35 m, but decreasing in amplitude towards the bottom. (c) The gradient Richardson number (Ri), which has been computed from ADCP and thermistor string data at the minimum possible vertical resolution, which is dictated by the thermistor separation. Below 30 m depth, ISl , and hence low Ri , are dominated by *tidal* current shear. Above this depth they are almost entirely determined by *inertial* current shear, with a transition zone between 25–30 m depth, where tidal current shear also contributes. Of our concern here are the Ri values between 10–22 m depth, where shear magnitudes reach up to $ISl = 15 \text{ cm s}^{-1} \text{ m}^{-1}$ during periods when isotherms are densely packed, such as around day 196.5 near 22 m depth. At those depths, low Ri are not only dominated by low N , as between 25–30 m depth, but also by relatively high ISl . Conversely, the band of $Ri > 1$ just above the lower thermocline is due to low ISl rather than high N . When *only* the near-inertial currents are removed from the ADCP records using a sharp harmonic filter, $Ri > 1$ above 25 m depth, *always*.

mixing, despite the strong stratification, which apparently attracts equally strong current shear. This inference of marginal instability follows from theoretical and numerical considerations on the transition between the stable (high Ri) and unstable (low Ri) regimes. A value of $Ri = 0.25$ is given

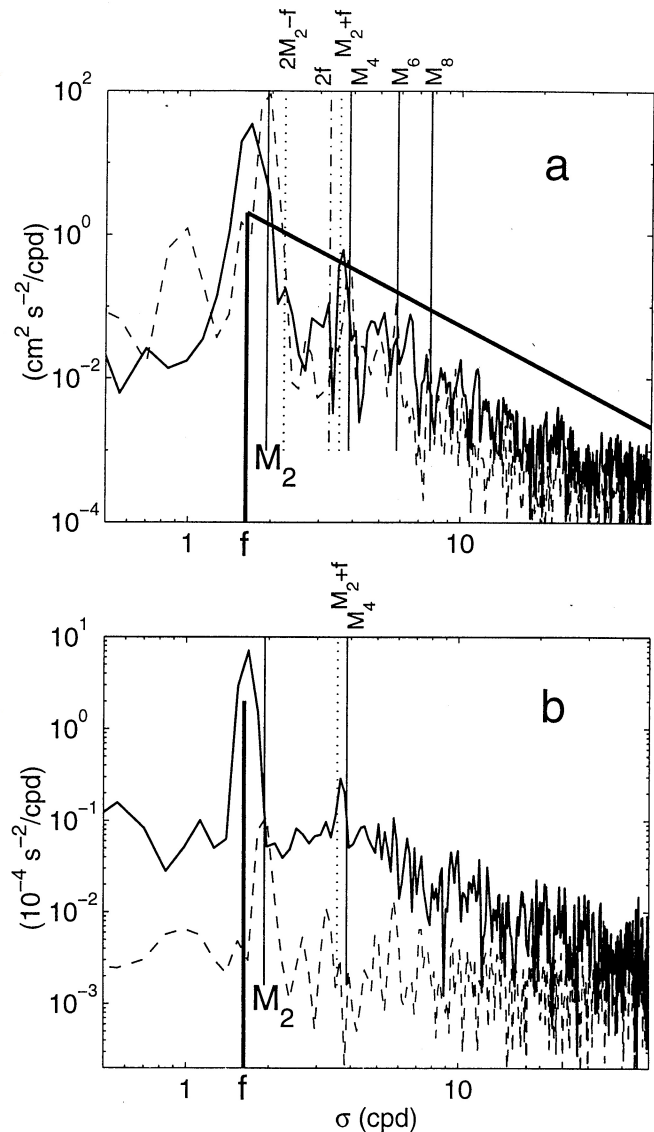


Figure 2. (a) Kinetic energy frequency spectra from baroclinic currents at 17 m depth (solid line) and barotropic currents (dashed line), observed in summer. These ‘barotropic’ currents exclude the frictionally induced near-bottom layer, and the near-surface layer which the ADCP did not resolve properly. The number of degrees of freedom (of about 3) is kept low to resolve some of the harmonic (M_2 , f) frequencies, at the expense of a high-accuracy error estimate. Hereby we do not disregard the appropriate statistics usually invoked, but we consider the strongest internal waves as deterministic rather than being a particular realization of a stochastic process, when monitored over a week. A simple graphic display of the canonical internal wave spectrum, showing the σ^2 decay, is given by the solid line between the frequencies f and N (outside the graph, not indicated). The thin vertical solid lines indicate M_2 and its higher harmonics, the dash-dotted line the first harmonic of the inertial frequency, and the dotted lines composite frequencies of M_2 . (b) Shear spectra by finite differencing over 0.5 m intervals current observations near 13 m depth (solid line) and, for comparison, near 40 m depth, in the frictionally sheared bottom boundary layer (dashed line).

for such transition following *linear* stability theory [Miles and Howard, 1964]. However, a transition value of $Ri \approx 1$ is suggested [Holloway, 1983; Abarbanel et al., 1984] for a breakdown of a *non-linear* flow, for example through interaction of two spatially and temporally varying currents.

The distribution of $0.25 < Ri < 1$ we observed during a prolonged period of *calm* weather suggests that the occurrence of enhanced vertical mixing is likely to occur *across* the stratification rather than in the weakly stratified layers in between. An indirect estimate to quantify this mixing is obtained from small temperature inversions apparent in high resolution CTD profiles with depth [Thorpe, 1987]. Using the available 12 CTD profiles spread over days 194–199, we computed an average value of $K = (3 \pm 2) \times 10^{-5} \text{ m}^2 \text{ s}^{-1}$ with peak values up to $K = 6 \times 10^{-4} \text{ m}^2 \text{ s}^{-1}$ at depths where stratification is relatively large ($N(z) > 0.025 \text{ s}^{-1}$). This excluded occasional temperature inversions in stable intrusions, found in weaker stratified layers only.

Statistically, the observed distribution of Ri favours low Ri in layers of high N and, within such layers, a tendency for high shear anomalies driving Ri critical, as found for the abyssal ocean [Pinkel and Anderson, 1997]. We find $N^2 = [(0.15 \pm 0.05)|S|^2 + (1 \pm 0.5)] \times 10^{-3} \text{ s}^{-2}$, indicating a background stratification without shear and a rate smaller than $Ri = 0.25$. Such relationship is also observed in the abyssal ocean at parameter values two orders of magnitude lower, yielding, remarkably, almost identical slope and similar cut-off [Fig. 8 in Polzin, 1996]. Associated turbulence dissipation rates were successfully modelled with a transition criterion of $Ri_c = 0.4$. The dependence between $|S|^2$ and N^2 was attributed to the effects of turbulent fluxes and internal waves interacting with buoyancy perturbations [Polzin, 1996].

We hypothesize that this (occasional) mixing across strong stratification is *internally driven* by near-inertial current shear, in interaction with high frequency (breaking) internal waves, which are found in the internal wave frequency (σ) domain $f < \sigma < N$. This is inferred from the distribution of high frequency internal wave energy ($\sigma > 2f$), which is also organized near the thermoclines and, hence, near the regions of enhanced shear and low Ri . As will be discussed below, these high-frequency internal waves themselves are the result of nonlinear interaction between inertial motions and tidal currents, which not only has its influence on the mixing across stratification, but also on the particular form of the

internal wave spectrum, with its canonical [Garrett and Munk, 1972b] decay rate of σ^{-2} in the frequency domain.

In order to obtain the internal wave spectrum we split the current observations at each depth in two parts, a 'barotropic' part $\langle u \rangle = -_{35}f^{10} u \, dz/25$, depths in m and similar for v , and the remainder, 'baroclinic' part containing the internal waves [Figure 2(a)]. The barotropic current spectrum is dominated by the tidal and its harmonic frequencies (M_4, M_6, M_8). In contrast, the major part of the energy in the internal wave spectrum is contained near the inertial frequency at depths where $N(z)$ is large and a remarkable enhancement is found at about 3.5 cpd. This frequency is not the first harmonic of the near-inertial frequency, but a composite (M_2+f) of tidal and inertial frequencies. This indication for non-linear interaction between (near)-inertial waves and tidal currents is supported by the enhancement at other interaction frequencies, like at 2.2 cpd ($2M_2-f$). The driving mechanism, the vertical current shear, shows a spectral increase upto $\sigma \approx 10f$, with enhanced peaks near the inertial and M_2+f frequencies, and *not* at the tidal frequency [Figure 2(b)]. The shear spectrum retains these features in a semi-Lagrangian frame of reference, indicating that the enhancement at the interaction frequencies is not due to vertical advection [Sherman and Pinkel, 1991]. Note that, as the shear is predominantly generated by inertial motions which are inherently circularly (anti-cyclonically) polarized, the shear *magnitude* is essentially constant with time. Inertial motions generate 'maximal shear' by having their individual current components 180° out-of-phase across each major thermocline, due to their extreme sensitivity to vertical momentum exchange [Maas and van Haren, 1987].

Discussion

Our observations support recent numerical evidence [Hibiya et al., 1996; Niwa and Hibiya, 1997] and ocean observations [Mihaly et al., 1998] on the importance of near-inertial motions in internal wave band energy transfer, which also confirmed earlier suggestions [Holloway, 1980, 1983] that internal wave interaction is likely strong. This is reflected in a near-constant $Ri \approx 1$, as observed [Figure 1(c)], and it may explain the consistency of the internal wave spectrum [Munk, 1981]. We infer this from a slight smoothing of the nearly raw spectra presented here [Figure 2(a)], which rapidly leads to a collapse from enhanced energy at localized

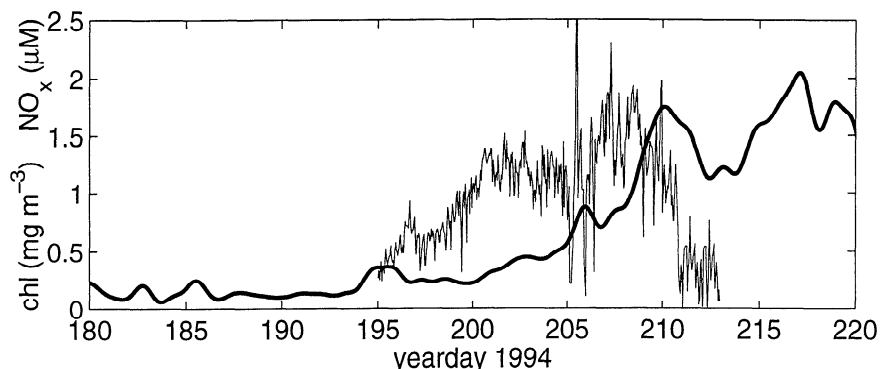


Figure 3. Hourly observations from 13 m depth of nutrients from an in-situ auto-analyzer (NO_x , thin line) and chlorophyll from fluorometer data (chl, daily filtered, thick line). Despite a favourable light regime in summer, the phytoplankton contents in the near-surface layer are very low, due to lack of nutrients, until the moment of renewed nutrient input, which is generally thought not to occur until the first late-summer storm.

interaction frequencies to a uniform σ^{-2} -decay in frequency and, when scaled with the local buoyancy frequency, to a fixed level to within a factor of two, as in deep ocean data [Fofonoff and Webster, 1971].

The overall picture that emerges is a subtle balance between the (rapidly varying) stratification rate, near-inertial shear, and high-frequency internal waves, down to a well organized criticality, imposed by the sun and the atmosphere. Given the universality of the internal wave spectrum, the 'constant' relationship between stratification rate and shear through $Ri \approx 1$ implies stratification provoking mixing, or the reverse, mixing leading to stratification [Thompson, 1979]. In practice, this may help to identify ocean regions where internal wave energy is enhanced as, for example, due to focusing [Maas et al., 1997], by simply mapping the stratification rate. In (future) modelling, exchange across stratification should be parametrized from the monitoring of either one of (properly resolved) quantities N or $|S|$, together with a realistic generation of inertial motions.

We suggest that internal wave breaking is the only possible mechanism causing the observed replenishment of nutrients in the near-surface layer from below in mid-summer [Figure 3], ruling out advection by lack of a significant tidal spectral peak in these nutrients. The associated bloom of phytoplankton, typically peaking 4-5 days later, occurred under calm weather conditions well before the first late-summer storm (on day 223), when surface and bottom mixed layers became separated by a single, thin thermocline. This bloom could not be mimicked by existing numerical models on vertical exchange across a pycnocline, lacking internal waves [Ruardij et al., 1997].

Acknowledgements. We greatly appreciate the assistance of the crew of the R.V. Pelagia during the Integrated North Sea Programme (INP). Hendrik van Aken suggested the split of the currents. During INP, HvH was supported by a grant from the Netherlands organisation for the advancement of scientific research, NWO.

References

- Abarbanel, H.D.I., D.D. Holm, J.E. Marsden, and T. Ratiu, Richardson number criterion for the nonlinear stability of three-dimensional stratified flow, *Phys. Rev. Lett.*, **52**, 2352-2355, 1984.
- Fofonoff, N.P., and F. Webster, Current measurements in the western Atlantic, *Phil. Trans. R. Soc. Lond.*, **A270**, 423-436, 1971.
- Garrett, C., and W. Munk, Oceanic mixing by breaking internal waves, *Deep-Sea Res.*, **19**, 823-832, 1972a.
- Garrett, C.J.R., and W.H. Munk, Space-time scales of internal waves, *Geophys. Fluid Dyn.*, **3**, 225-264, 1972b.
- Gregg, M.C., and E. Kunze, Shear and strain in Santa Monica Basin, *J. Geophys. Res.*, **96**, 16709-16719, 1991.
- Hibiya, T., Y. Niwa, K. Nakajima, and N. Sugimoto, Direct numerical simulation of the roll-off range of internal wave shear spectra in the ocean, *J. Geophys. Res.*, **101**, 14123-14129, 1996.
- Holloway, G., Oceanic internal waves are not weak waves, *J. Phys. Oc.*, **10**, 906-914, 1980.
- Holloway, G., A conjecture relating oceanic internal waves and small-scale processes, *Atmos.-Ocean*, **21**, 107-122, 1983.
- Maas, L.R.M., D. Benielli, J. Sommeria, and F.-P.A. Lam, Observation on an internal wave attractor in a confined, stably stratified fluid, *Nature*, **388**, 557-561, 1997.
- Maas, L.R.M., and J.J.M. van Haren, Observations on the vertical structure of tidal and inertial currents in the central North Sea, *J. Mar. Res.*, **45**, 293-318, 1987.
- Mihaly, S.F., R.E. Thomson, and A.B. Rabinovich, Evidence for nonlinear interaction between internal waves of inertial and semidiurnal frequency, *Geophys. Res. Lett.*, **25**, 1205-1208, 1998.
- Miles, J.W., and L.N. Howard, Note on a heterogeneous shear flow, *J. Fluid Mech.*, **20**, 331-336, 1964.
- Munk, W., Internal waves and small-scale processes, in *Evolution of physical oceanography*, edited by B.A. Warren, and C. Wunsch, pp. 264-291, MIT Press, Cambridge, MA, 1981.
- Munk, W.H., and E.R. Anderson, Notes on a theory of the thermocline, *J. Mar. Res.*, **7**, 276-295, 1948.
- Niwa, Y., and T. Hibiya, Nonlinear processes of energy transfer from travelling hurricanes to the deep ocean internal wave field, *J. Geophys. Res.*, **102**, 12469-12477, 1997.
- Pinkel, R., and S. Anderson, Shear, strain, and Richardson number variations in the thermocline. Part I: statistical description, *J. Phys. Oc.*, **27**, 264-281, 1997.
- Polzin, K., Statistics of the Richardson number: mixing models and finestructure, *J. Phys. Oc.*, **26**, 1409-1425, 1996.
- Ruardij, P., H. van Haren, and H. Ridderinkhof, The impact of thermal stratification on phytoplankton and nutrient dynamics in shelf seas: a model study, *J. Sea Res.*, **38**, 311-331, 1997.
- Sherman, J.T., and R. Pinkel, Estimates of vertical wave-number-frequency spectra of vertical shear and strain, *J. Phys. Oc.*, **21**, 292-303, 1991.
- Thompson, R.O.R.Y., A mechanism for angular momentum mixing, *Geophys. Astrophys. Fluid Dyn.*, **12**, 221-234, 1979.
- Thorpe, S.A., Current and temperature variability on the continental slope, *Phil. Trans. R. Soc. Lond.*, **A323**, 471-517, 1987.
- Turner, J.S., *Buoyancy effects in fluids*, 368 pp., Cambridge Univ. Press, Cambridge, UK, 1979.

H. van Haren, L. Maas, J.T.F. Zimmerman, H. Ridderinkhof and H. Malschaert, Netherlands Institute for Sea Research (NIOZ), P.O. Box 59, 1790 AB Den Burg, the Netherlands.
(e-mail: hansvh@nioz.nl)

(Received May 14, 1999; revised August 02, 1999; accepted August 18, 1999.)